Am J Transl Res 2018;10(8):2555-2566
www.ajtr.org /ISSN:1943-8141/AJTR0072538

Original Article

Apoptosis of bone marrow mesenchymal stromal/stem cells via the MAPK and endoplasmic reticulum stress signaling pathways

Tielong Chen, Houyong Zhu, Yu Wang, Pengjie Zhao, Jingyu Chen, Jing Sun, Xiudong Zhang, Guangli Zhu

Department of Cardiology, Hangzhou Hospital of Traditional Chinese Medicine, Hangzhou, China

Received January 11, 2018; Accepted July 22, 2018; Epub August 15, 2018; Published August 30, 2018

Abstract: Therapy for myocardial regeneration using bone marrow stromal cells (BM-MSCs) has been applied to improve the cardiac function of subjects with acute myocardial infarction. However, the study of this therapy has encountered a bottleneck because BM-MSCs are prone to apoptosis in ischemic and anoxic environments. The goal of this study was to investigate the expression of mitogen activated protein kinase (MAPK) (p-38, JNK and ERK) and endoplasmic reticulum stress protein (caspase-12 and CHOP) during BM-MSC apoptosis. In a BM-MSC model of hypoxia and serum deprivation (H/SD), we observed the morphology and apoptotic rate of BM-MSCs for 24 h and found that the nuclear shrinkage and apoptosis rate increased gradually and reached a maximum apoptosis rate at the 6 h time point. Then, with the prolongation of the hypoxia time, the number of nuclear shrinkage cells and the apoptosis rate gradually decreased. The expression levels of p-38, JNK, ERK, procaspase-12, caspase-12 and CHOP increased at each H/SD time point. In addition, compared with the H/SD 6 h group, the nuclear shrinkage and apoptosis rate were decreased in the SB202190 and SP600125 groups but increased in the PD98059 group. Further, the expression of caspase-12 in the SB202190 group decreased, while the expression of procaspase-12 increased, compared with the H/SD 6 h group. Overall, our findings suggested that p-38, JNK, CHOP and caspase-12 play important roles in promoting the apoptosis of BM-MSCs, while ERK is contrary to other signals. Moreover, the apoptosis of BM-MSCs was induced by H/SD via the p-38-caspase-12 signaling pathway.

Keywords: Bone marrow stromal cells, apoptosis, mitogen activated protein kinase, endoplasmic reticulum stress, p-38, JNK, ERK, procaspase-12, caspase-12, CHOP

Introduction

Left ventricular remodeling caused by myocardial cell loss and irregular fibrous proliferation seriously affect the recovery of cardiac function after acute myocardial infarction (AMI) [1-4]. Myocardial cell regeneration is a newly developed cell therapy that transplants stem cells into areas where the heart is depressed, instead of ischemic and anoxic myocardium. Both experimental and clinical studies have shown that stem cell transplantation can improve cardiac function and promote angiogenesis [5-10]. Currently, bone marrow mesenchymal stromal/stem cells (BM-MSCs) have attracted great attention from researchers because of their strong plasticity and self-availability [11, 12]. However, it has recently been found that, when BM-MSCs are transplanted into infarcted myocardium after AMI, most of the BM-MSC apoptosis occurs in the microenvironment of ischemia and hypoxia, affecting the therapeutic effects of BM-MSCs transplantation [13, 14]. Therefore, it is important to prevent BM-MSCs from apoptosis in the harsh microenvironment of ischemia and hypoxia.

Recent studies have shown that endoplasmic reticulum stress (ERS) plays an important role in many cell apoptosis processes [15-17]. Early ERS is a response promoting survival, while the unfolded protein response reduces the accumulation of unfolded protein and restores the function to the endoplasmic reticulum. However, when the unfolded protein response is not sufficient to protect cell survival, the endoplasmic reticulum will act as the trigger point of apoptosis signals to induce apoptosis and promote the

expression of apoptosis-inducing factors, such as the caspase family and C/EBP homologous protein (CHOP). The caspase family is a key molecular group for apoptosis. By cutting off contact with the surrounding cells, caspase family members can recombine the cytoskeleton, shut down DNA replication, destroy DNA and nuclear structures, and induce the formation of apoptotic bodies, in which caspase-12 is closely related to ERS [18]. CHOP, as an ERS-specific transcription factor, plays an important role in endoplasmic reticulum stress-induced apoptosis [18, 19]. However, the status and specific molecular mechanisms of caspase-12 and CHOP are not clear in the process of BM-MSC apoptosis.

Mitogen-activated protein kinase (MAPK), a serine/threonine protein kinase, can transduce extracellular signals into cells and their nuclei and can regulate gene expression through the activation of transcription factors via a conserved three stage cascade (MAPKKK-MAPKK-MAPK). This pathway might be involved in many physiological processes, such as cell movement, apoptosis, differentiation and proliferation. The subgroup mainly includes the extracellular signal-regulated kinase (ERK) signaling pathway, c-Jun N-terminal kinase (JNK) signaling pathway, and p-38 signaling pathway [20, 21]. ERK was the first member of the MAPK family to be discovered and extensively studied. It has the potential to promote cell survival and anti-apoptosis, and it is considered a classic cell protective signaling pathway [22, 23], while activation of JNK and p-38 has generally been associated with the promotion of apoptosis [24-26]. Therefore, in this study, we also investigated whether MAPK plays an important regulatory role in the apoptosis of BM-MSCs.

The aim of this experiment was to investigate the changes in the MAPK family and ERS during BM-MSC apoptosis, as well as to investigate whether there is an inherent relationship between the MAPK family and ERS in regulating the apoptosis of BM-MSCs.

Materials and methods

Chemicals and reagents

Adult male Sprague-Dawley (SD) rats (70-90 g) were acquired from the Laboratory Animal Center of Zhejiang Chinese Medical University Laboratory Animal Research Center (certificate number SYXK (Zhe) 2013-0184). Low glucose Dulbecco's Modified Eagle's Medium (DMEM), glucose-free DMEM, 0.25% trypsin of 0.02% EDTA, and phosphate-buffered saline (PBS) were acquired from Gino Biological Medical Technology Co., Ltd. (Zhejiang, China). Fetal bovine serum (FBS) and bovine serum albumin (BSA) were acquired from Zhejiang Tianhang Biological Technology Co., Ltd. (Zhejiang, China). Protein phosphatase inhibitor mixture, protease inhibitor mixture, and SDS-PAGE protein sample buffer were acquired from Darwin Biotechnology Company. (Zhejiang, China). Anti-rat CD44H PE, anti-rat CD45 PE, and anti-mouse/rat CD90 FITC were acquired from Thermo Fisher Scientific (Waltham, MA, USA). Hoechst 33342 fluorescent dye was acquired from Shanghai Jia Shi Science Instrument Co., Ltd. (Shanghai, China). The Annexin V-FITC&PI Apoptosis Kit was acquired from Biouniquer Company (Jiangsu, China). RIPA lysis buffer, BSA protein quantitative standard, and the protein quantitative kit were acquired from Beijing Pulilai Gene Technology Co., Ltd. (Beijing, China). Total p-38 (t-p-38), total JNK (t-JNK), total ERK (t-ERK), CHOP polyclonal antibody, and GAPDH polyclonal antibody were acquired from Protein tech Group, Inc. (Chicago, IL, USA). Caspase-12 (M-108): sc-5627 was acquired from Santa Cruz Biotechnology. (Dallas, TX, USA). Anti-JNK1+JNK2+JNK3 (phospho Y185+Y185+Y223) antibody, anti-p-38 (phospho T180) antibody, and anti-Erk1 (pY204)+Erk2 (pY187) antibody were acquired from Abcam Company (Cambridge, UK). SB202190, SP6-00125, and PD98059 were acquired from Selleck Chemicals. (Houston, TX, USA). Enhanced bicinchoninic acid (BCA) and the protein assay kit were acquired from Beyotime (Jiangsu, China).

Extraction and culture of BM-MSCs from rats

Two male SD rats were sacrificed and sterilized for 2 min in a beaker containing 75% alcohol. The femur and tibia were removed on an aseptic operating table (Suzhou Purification, Jiangsu, China). The ends of the femur and tibia were severed, and the bone marrow cavities were repeatedly aspirated using sterile syringes containing 10% FBS complete culture medium until the bone marrow cavities were white; then, the bone marrow culture medium was transferred to the cell culture dish and cultured at 37°C in

a 5% CO_2 and 95% saturated humidity incubator (Thermo, Waltham, MA, USA). After 24 h, the culture medium was replaced, the suspension of dead cells was removed, fresh intact medium was added, and the liquid was changed once every two days. The cell state and fusion degree were observed at a fixed time every day under an inverted phase contrast microscope (Olympus, Tokyo, Japan). When the cells grew to 80%, the culture medium was removed and washed with PBS 2 times, and then the trypsin was added to lyse the cells in a 37°C incubator. When the cells became round, and the space between the cells increased, the trypsin was aspirated and discarded. Further, the 10% FBS DMEM complete medium was joined immediately to terminate digestion. Then, the cells were mixed and separated into a single cell suspension, inoculated into a new culture dish at a ratio of 1:2, and continued to be cultured at 37°C in a 5% CO_2, 95% saturated humidity incubator for subsequent experiments.

Identification of BM-MSCs

In the third passage (P3) generation, the well growing cells were digested by 0.25% trypsin and then centrifuged at 1000 r for 5 min at 4°C. The monoclonal antibodies CD44, CD45 and CD90 were added to each tube. At the same time, each tube sample was established with the same type negative control, and they were incubated on ice for 45 min. Then, flow cytometry (Beckman, Fullerton, CA, USA) was used for detection and analysis.

Establishment of the apoptosis model of BM-MSCs

The P3 generation of BM-MSCs was divided into five groups: control; hypoxia and serum deprivation 3 h (H/SD 3 h); hypoxia and serum deprivation 6 h (H/SD 6 h); hypoxia and serum deprivation 12 h (H/SD 12 h); and hypoxia and serum deprivation 24 h group (H/SD 24 h). In addition to the control group with low glucose DMEM and 10% FBS, the other groups were replaced with glucose free and serum free DMEM and were placed in anaerobic culture medium for 3 h, 6 h, 12 h, and 24 h, respectively. The above groups were cultured at 37°C in 5% CO_2. Then, each group was stained with Hoechst 33342 to determine the best modeling time using a fluorescence microscope (Olympus, Tokyo, Japan), as well as stained with Annexin V-PI to observe the cell apoptosis using flow cytometry.

Changes in MAPK and ERS proteins during BM-MSC apoptosis

The P3 generation of BM-MSCs was divided into four groups: control; hypoxia and serum deprivation 2 h (H/SD 2 h); hypoxia and serum deprivation 4 h (H/SD 4 h); and H/SD 6 h. Then, the hypoxia group was submitted to the corresponding hypoxic treatment as before. Western blotting was performed to analyze the changes in MAPK and ERS protein. Briefly, each group of cells was collected and split for 30 min in an ice bath. The pyrolysis product was centrifuged at 12000 g for 15 min, and then the suspension was collected. The protein concentration (30 μg) was determined by BCA assay and UV spectrophotometer (Thermo, Waltham, MA, USA). Protein was denatured in a heating block at 100°C for 10 min. The samples were electrophoretically separated by SDS-PAGE and were transferred to polyvinylidene fluoride sheets using a transblot apparatus. Membranes were blocked for 90 min at room temperature with 5% BSA dissolved in TBS-T buffer (25 mM Tris, 0.8% NaCl, 0.02% KCl and 0.1% Tween-20, pH 7.4). Samples were analyzed for p-p-38, p-JNK, p-ERK, procaspase-12, caspase-12, CHOP and GAPDH using the appropriate primary and secondary antibodies. Subsequently, the membranes of the first three were stripped and reprobed for t-p-38, t-JNK and t-ERK to normalize the p-p-38, p-JNK and p-ERK band intensities, respectively.

Effect of the MAPK signaling pathway on the apoptosis of BM-MSCs

BM-MSCs were divided into five groups: control; H/SD 6 h; SB202190 pretreatment (SB202190); SP600125 pretreatment (SP600125); and PD98059 pretreatment (PD98059). The control group was cultured with low glucose DMEM and 10% FBS, and the SB202190, SP600125 and PD98059 pretreatment groups were pretreated with 15 μm SB202190, 20 μm SP600125 and 100 μm PD98059, respectively, for 2 h (respectively blocking the p-38, JNK and ERK pathways); then, they were treated with 6 h of hypoxia with the H/SD 6h group as before. Each group was treated with Hoechst 33342 staining and Annexin V-PI staining to observe the apoptosis levels of BM-MSCs qualitatively and quantitatively.

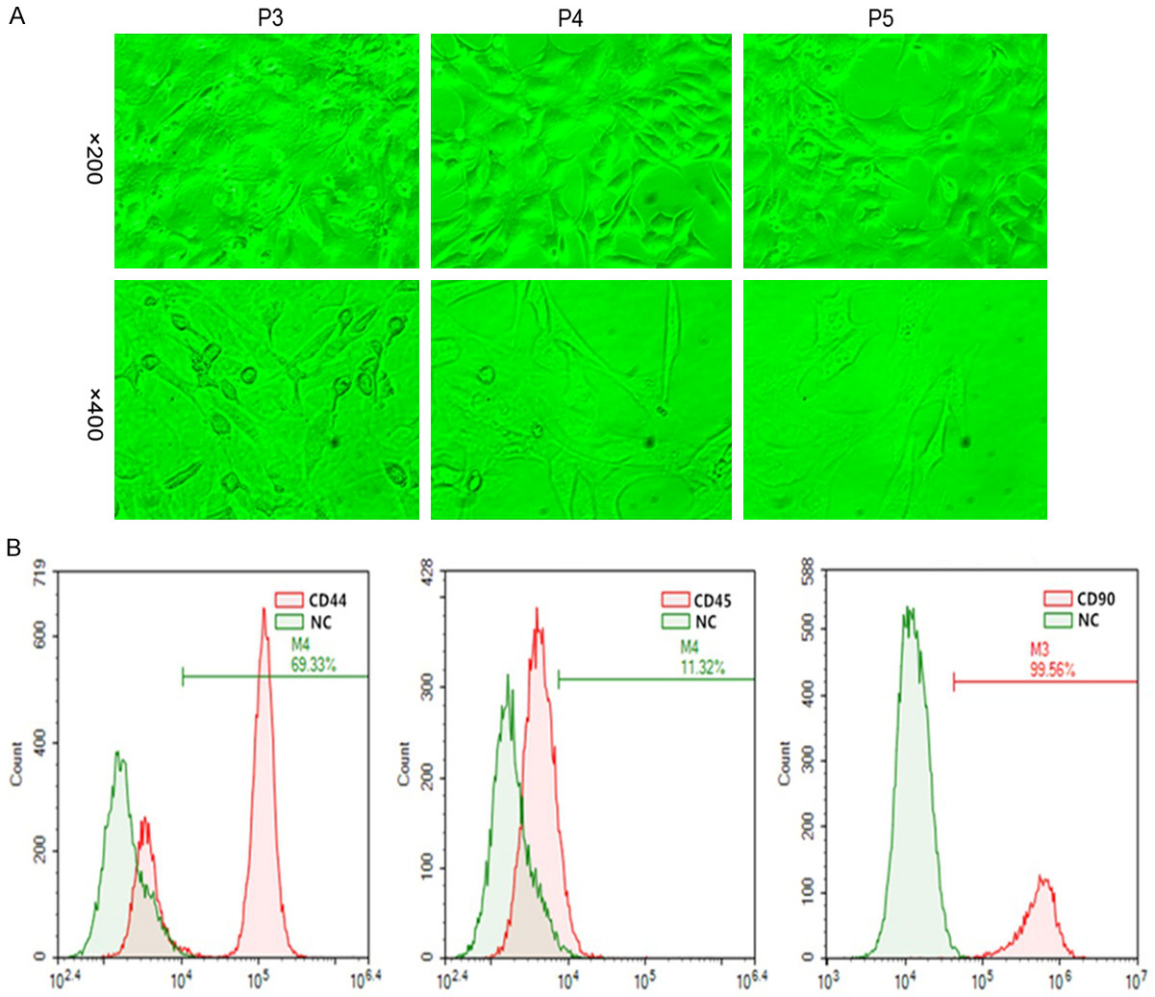

Figure 1. Identification of qualified BM-MSCs. A. Morphological observation (magnification, 1 = ×200, 2 = ×400). The P3 generation of BM-MSCs had uniform morphology, spindle shapes or long spindle shapes and were arranged in an orderly manner, and the number of hybrid cells decreased significantly. B. Detection of specific indicators of qualified BM-MSCs by flow cytometry in the P3 generation. Flow cytometry also showed that the specific positive indicators of CD44 and CD90 were highly expressed in the P3 generation, while the negative index CD45 was minimally expressed.

Correlation between MAPK and ERS protein

BM-MSCs were divided into four groups: control; H/SD 6 h; SB202190; and SP600125. Each group was pretreated and treated with hypoxia and then analyzed by western blotting, as above.

Statistical analysis

All of the values are expressed as the mean ± S.E.M. Statistical analysis was performed with SPSS software, version 19 (SPSS Inc., Chicago, IL, USA). Significant differences were assessed by one way analysis of variance, followed by the Student-Newman-Keuls test or Dunnett's post hoc test. Differences among the groups were considered significant at $P < 0.05$.

Results

Identification of BM-MSCs

We identified BM-MSCs by morphological observation and flow cytometry. Morphological observation showed that the P3 generation of BM-MSCs had uniform morphology, spindle shapes or long spindle shapes and were arranged in an orderly manner, and the number of hybrid cells decreased significantly that could be used for BM-MSC flow identification and subsequent experiments (**Figure 1A**). Flow

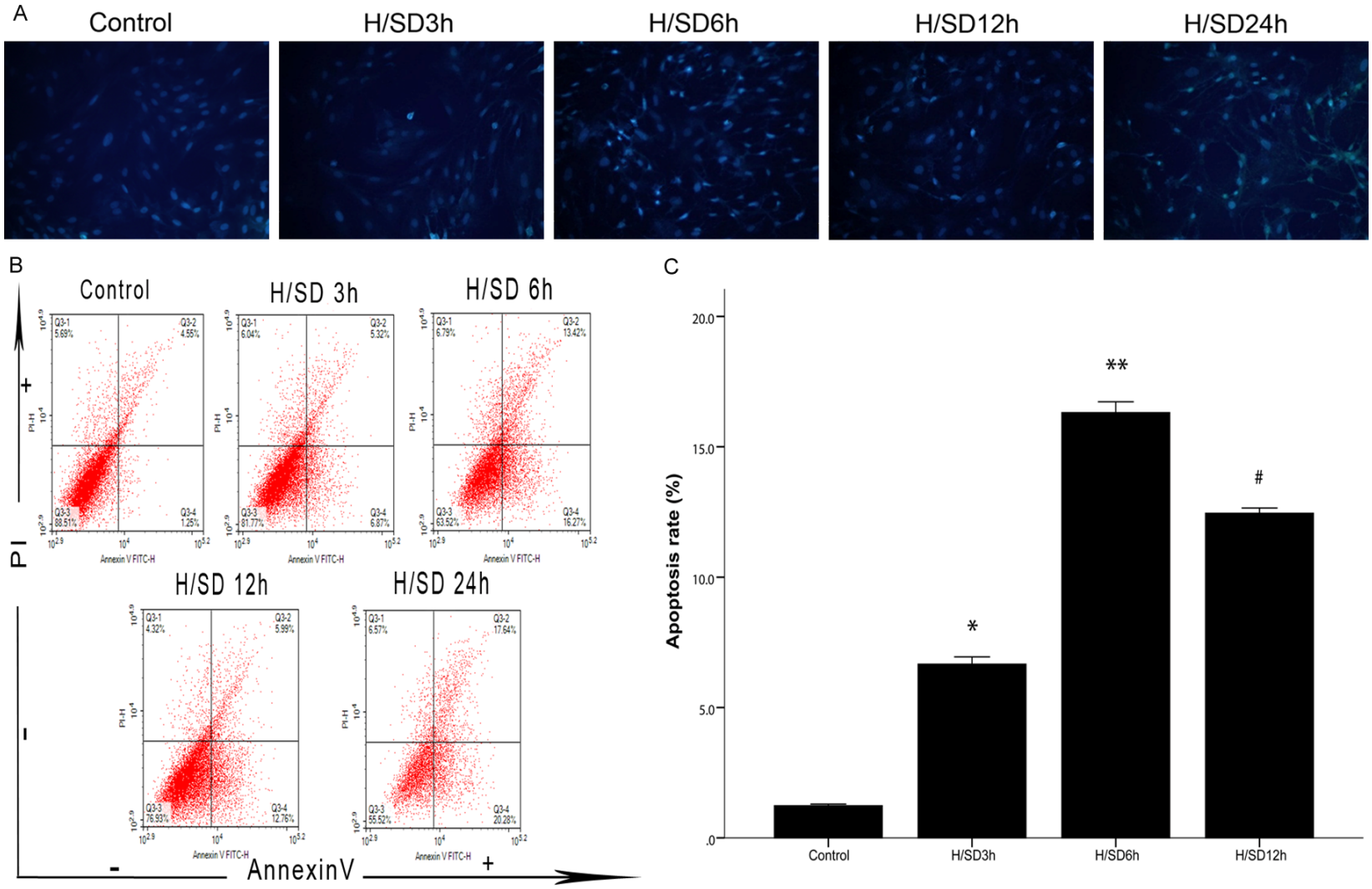

Figure 2. The changes in BM-MSC apoptosis levels at different time points of hypoxia and serum deprivation. A. BM-MSCs from the five groups with Hoechst 33342 staining (magnification, = ×200). In the H/SD groups, the apoptotic cells are dyed brighter because of nuclear crinkle compared to normal cells, the most obvious of which was the H/SD 6 h group. B. Annexin V-PI double staining flow cytometry for BM-MSC apoptosis. Annexin V^-/PI^- indicates normal cells, Annexin V^+/PI^- indicates early apoptotic cells, Annexin V^+/PI^+ indicates late apoptotic cells, and Annexin V^-/PI^+ indicates necrotic cells. C. Detection of apoptosis rate. Flow cytometry showed that the apoptosis rate of cells in each H/SD group was higher than that in the control group, and the rate of apoptosis in the H/SD 6 h group was the highest. All of the values are the mean ± S.E.M. (n = 3 per group). $^*P < 0.05$ vs control group, $^{**}P < 0.01$ vs control group. $^{\#}P < 0.05$ vs H/SD 6 h group.

cytometry also showed that the specific positive indicators of CD44 and CD90 were highly expressed in the P3 generation BM-MSCs (69.33% and 99.56%, respectively), while the negative index for CD45 was minimally expressed (11.32%) (**Figure 1B**).

Selection of apoptosis model of BM-MSCs

The establishment of the apoptosis model was evaluated by Hoechst 33342 staining and flow cytometry. Hoechst 33342 staining showed that, compared with the control group, the H/SD groups showed a unique morphology of cell apoptosis: nuclear shrinkage. The apoptosis rates of BM-MSCs at different time gradients under hypoxic conditions showed a certain trend; that is, from 0 h to 6 h, the nuclear shrinkage gradually increased and reached the maximum apoptosis rate at the 6 h time point. Then, with the extension of hypoxia time, the number of nuclear shrinkage cells gradually decreased (**Figure 2A**). Flow cytometry also showed that, compared with the control group, the apoptosis rate increased in the H/SD groups, the trend of apoptosis was consistent with the results of Hoechst 33342 staining, and the apoptosis rate of the H/SD 6 h group was the highest ($P < 0.05$) (**Figure 2B**, **2C**). Interestingly, according to the results of flow cytometry, the apoptosis rate of the H/SD 24 h group was higher than that of the H/SD 6 h group, but based on the number of cells surviving and the results of Hoechst 33342 staining, the cells in the H/SD 24 h group underwent necrosis, interfering with the accuracy of flow cytometry.

Activation of MAPK and ERS protein during the apoptosis of BM-MSCs

To investigate whether MAPK and ERS protein participate in the apoptosis of BM-MSCs, p-38, JNK, ERK, procaspase-12, caspase-12 and CHOP were detected by western blotting. After hypoxic preconditioning for 2 h, 4 h and 6 h, compared with the control group, the expression of p-38 in the H/SD groups increased at each time point ($P < 0.05$ for all, **Figure 3A**, **3B**), and the expression of the H/SD 2 h and H/SD 4 h groups increased obviously and reached a maximum at 4 h after hypoxia (both $P < 0.01$). Compared with the control group, the expression of JNK in the H/SD 2 h group did not change significantly, but the expression of the H/SD 4 h and H/SD 6 h groups increased ($P < 0.01$ and $P < 0.05$, respectively). Compared with the control group, the expression of ERK increased in all of the H/SD groups ($P < 0.05$ for all). The expression of procaspase-12 in the H/SD 4 h group increased compared with the control group ($P < 0.01$, **Figure 3C**, **3D**). The expression of caspase-12 in the H/SD 4 h group was increased compared with the control group ($P < 0.01$). Compared with the control group, the expression of CHOP in the H/SD groups increased significantly ($P < 0.01$ for all), and the expression increased gradually with the time gradient.

Regulation of the MAPK signaling pathway on apoptosis of BM-MSCs

To demonstrate the hypothesis that activation of the MAPK signaling pathway regulates apoptosis of BM-MSCs, rather than being an incidental phenomenon in BM-MSC apoptosis, we used SB202190, SP600125, and PD98059 to block the p-38, JNK, and ERK signaling pathways, respectively. Then, apoptosis was observed by Hoechst 3334 staining and flow cytometry to evaluate the role of the MAPK signaling pathway in regulating BM-MSC apoptosis. Hoechst 33342 staining showed that, compared with the control group, more BM-MSCs in the H/SD 6 h group showed a unique morphology of apoptosis and nuclear shrinkage, while the BM-MSCs showing nuclear shrinkage in the SB202190 and SP600125 groups decreased significantly, but the BM-MSCs showing nuclear shrinkage in the PD98059 group did not decrease significantly (**Figure 4A**). Flow cytometry showed that, compared with the H/SD 6 h group, the apoptosis rate of BM-MSCs in the SB202190 and SP600125 groups was significantly decreased (both $P < 0.05$, **Figure 4B**, **4C**), while the apoptosis rate in the PD98059 group was increased ($P < 0.05$).

Correlation between MAPK and ERS protein

To further investigate the relationship between MAPK and ERS protein, p-38, JNK, procaspase-12, caspase-12 and CHOP were detected by western blotting. Compared with the control group, the expression of caspase-12 in the H/SD 6 h group increased significantly ($P < 0.01$, **Figure 5A**, **5B**). Compared with the H/SD 6 h group, the expression of caspase-12 in the SB202190 group decreased significantly ($P <$

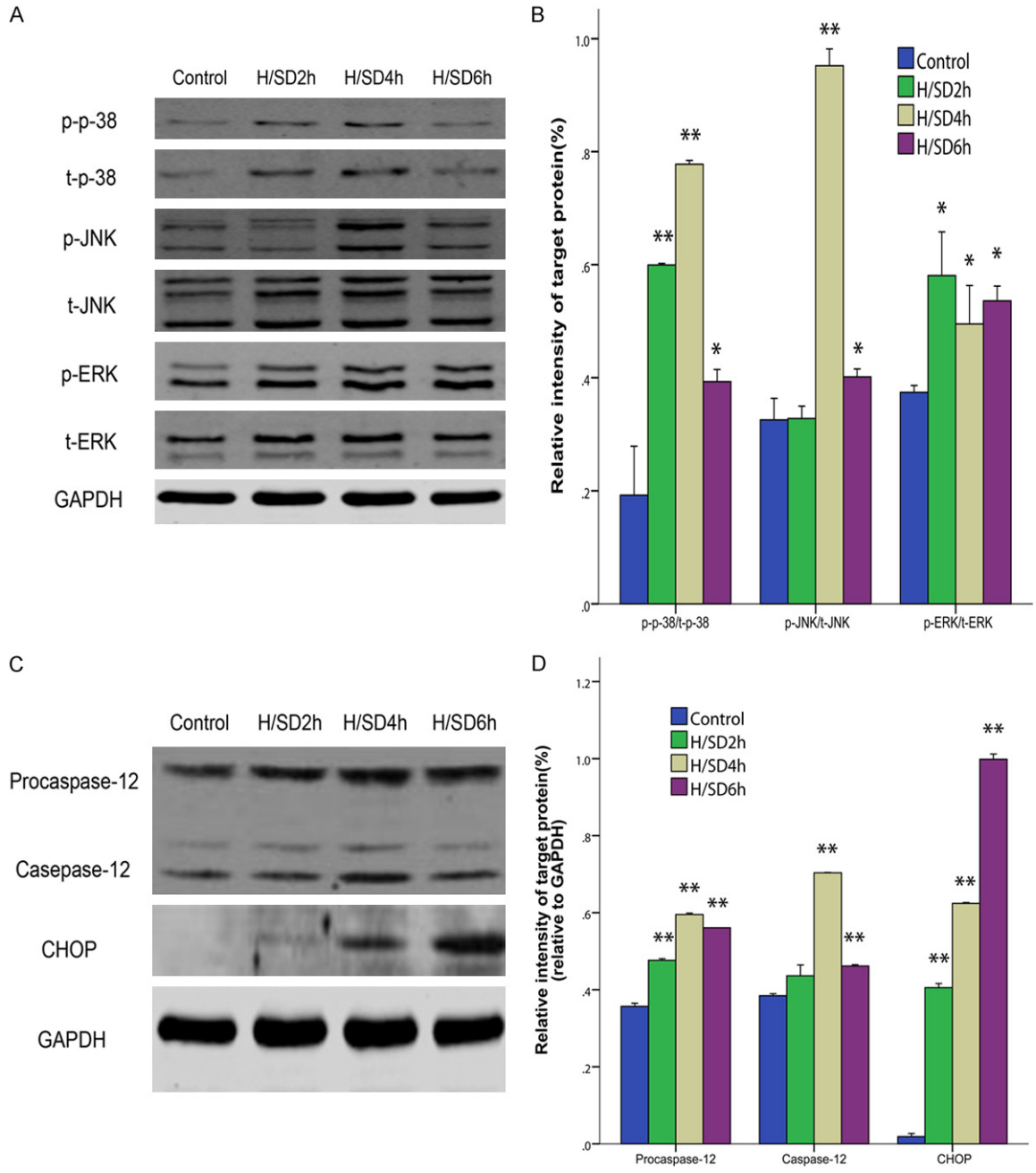

Figure 3. Expression of the phosphorylation of MAPK and ERS. A. Representative immunoreactive bands for phosphorylated p-38, JNK and ERK. B. The average of p-p-38/t-p-38, p-JNK/t-JNK and p-ERK/t-ERK. The phosphorylation rates of p-38, JNK and ERK increased after hypoxia and serum deprivation, and the phosphorylation rates of P-38 and JNK in the H/SD6 group were the highest. C. Representative immunoreactive bands for procaspase-12, caspase-12 and CHOP. D. The average of procaspase-12/GAPDH, caspase-12/GAPDH and CHOP/GAPDH. In addition to caspase-12 in H/SD 4 h group, the expression levels of procaspase-12, caspase-12 and CHOP increased after hypoxia and serum deprivation. All of the values are the mean ± S.E.M. (n = 3 per group). $^{*}P < 0.05$ vs control group. $^{**}P < 0.01$ vs control group.

0.01), while the expression of caspase-12 in the SP600125 group was not statistically significantly different ($P > 0.05$). Compared with the H/SD 6 h group, the expression of procaspase-12 in the SB202190 group decreased significantly ($P < 0.05$).

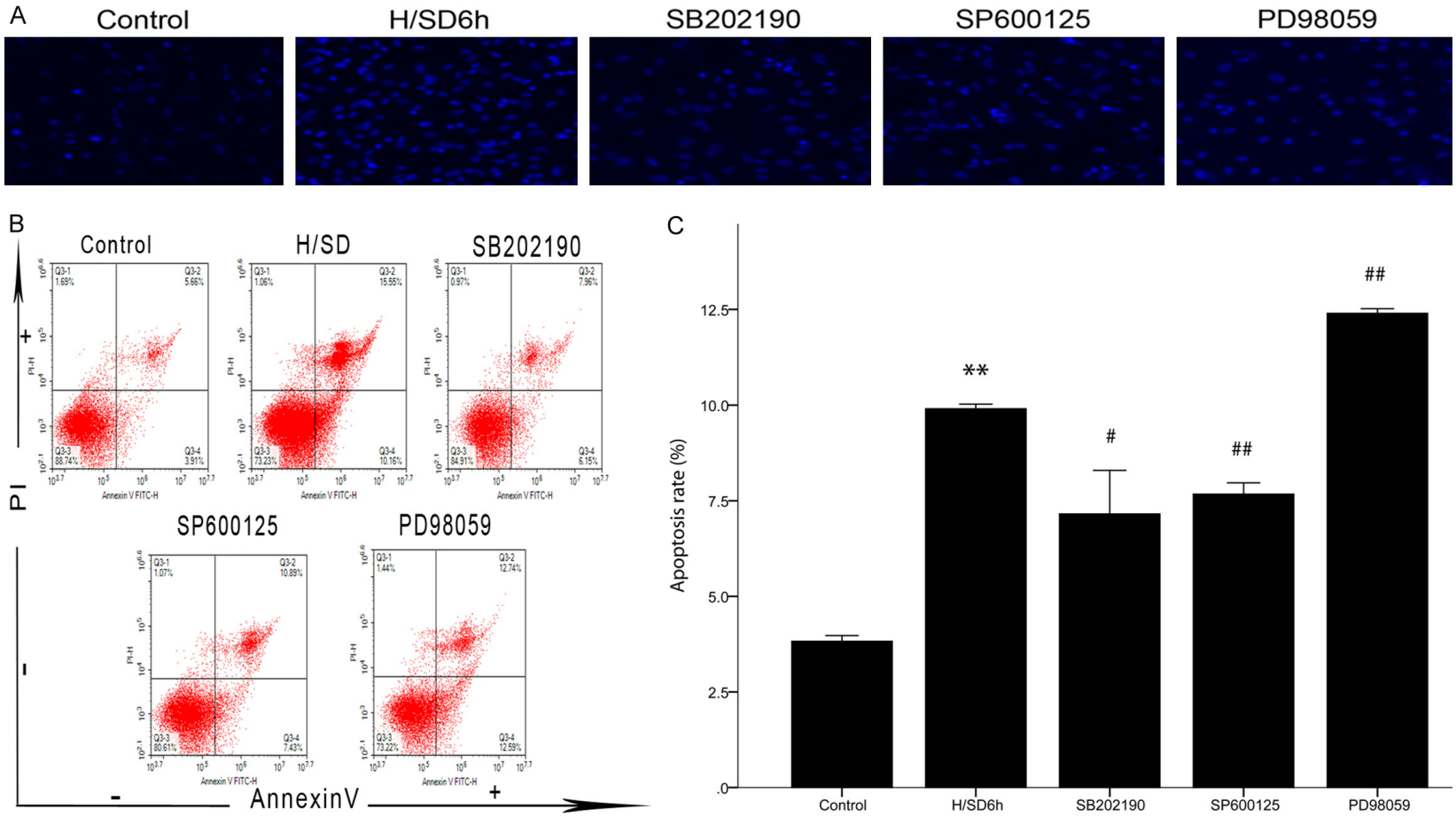

Figure 4. Regulation of the MAPK signaling pathway in the apoptosis of BM-MSCs. A. BM-MSCs from the five groups with Hoechst 33342 staining (magnification, = ×200). Compared with the H/SD 6 h group, the nuclear crumpled cells in the SB202190 and SP600125 groups decreased significantly, but the nuclear crumpled cells in the PD98059 group seemed to increase. B. Annexin V-PI double staining flow cytometry for BM-MSC apoptosis. Annexin V^-/PI^- indicates normal cells, Annexin V^+/PI^- indicates early apoptotic cells, Annexin V^+/PI^+ indicates late apoptotic cells, and Annexin V^-/PI^+ indicates necrotic cells. C. Detection of apoptosis rate. The apoptosis rate decreased after SB202190 and SP600125 intervention but increased after PD98059 intervention, compared with the H/SD 6 h group. All of the values are the mean ± S.E.M. (n = 3 per group). $^{**}P < 0.01$ vs control group. $^{\#}P < 0.05$ vs H/SD 6 h group. $^{\#\#}P < 0.01$ vs H/SD 6 h group.

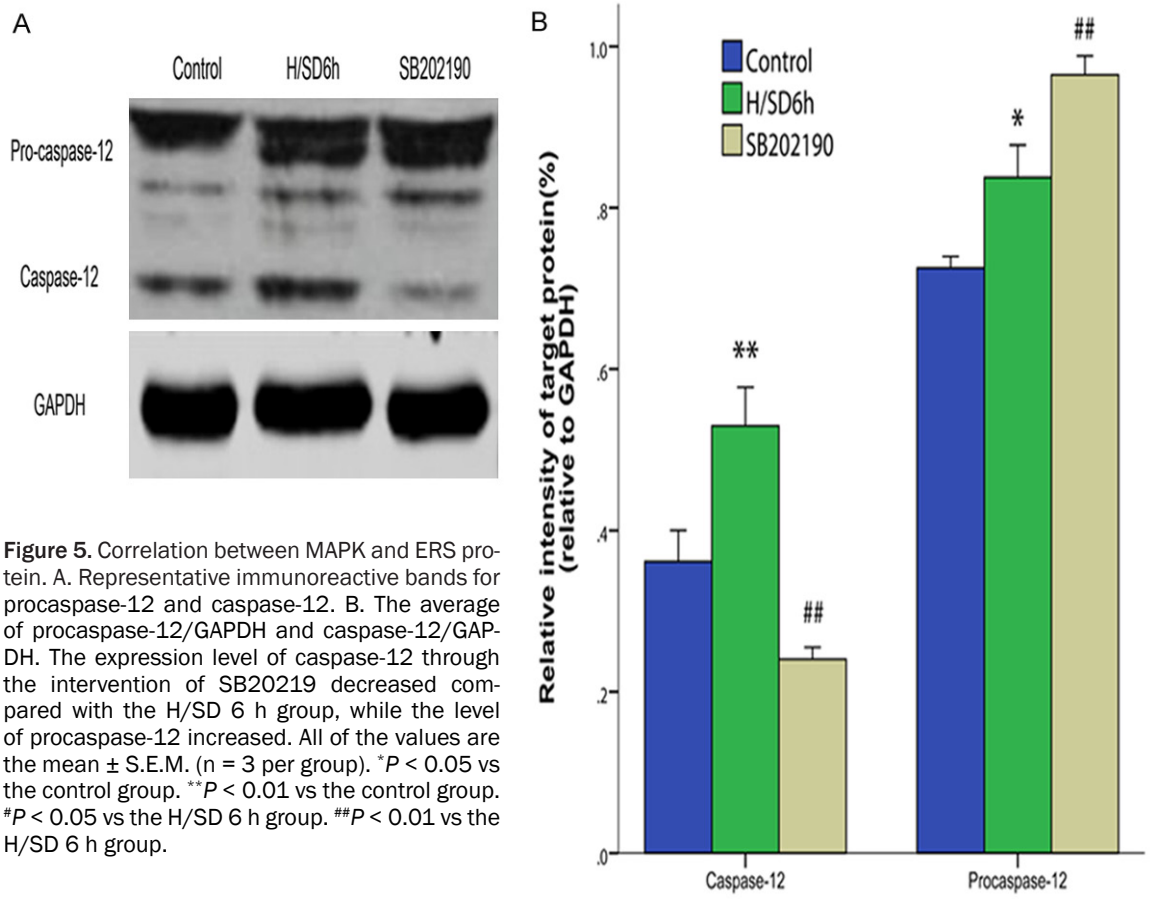

Figure 5. Correlation between MAPK and ERS protein. A. Representative immunoreactive bands for procaspase-12 and caspase-12. B. The average of procaspase-12/GAPDH and caspase-12/GAPDH. The expression level of caspase-12 through the intervention of SB20219 decreased compared with the H/SD 6 h group, while the level of procaspase-12 increased. All of the values are the mean ± S.E.M. (n = 3 per group). $^{*}P < 0.05$ vs the control group. $^{**}P < 0.01$ vs the control group. $^{\#}P < 0.05$ vs the H/SD 6 h group. $^{\#\#}P < 0.01$ vs the H/SD 6 h group.

Discussion

It is the premise of establishing an apoptosis model to extract and culture standard BM-MSCs. The flow cytometry identification of qualified BM-MSCs should meet the following criteria: 1) the surface specific markers CD44 and CD90 were detected to ensure the accuracy of cell selection; and 2) the negative index CD45 was detected to exclude the interference of hematopoietic cells [27, 28]. The results of this experiment showed that the expression of CD44, CD90 and CD45 met the standard of BM-MSC purification. In addition, the optimal BM-MSC apoptosis model was closely related to the hypoxia time. We found that the apoptotic rate of BM-MSCs showed a trend with time in the H/SD environment; that is, from 0 h to 6 h, the cell shrinkage or apoptosis rate increased gradually, and then with the extension of hypoxia time, the number of nuclear shrinking cells or the apoptotic rate gradually decreased. Therefore, we chose H/SD 6 h as the final time point for the observation of apoptosis.

Studies have shown that the endoplasmic reticulum plays an important role in the apoptosis of multiple cells [15-17]. Endoplasmic reticulum dysfunction can lead to ERS. Early ERS is a protective effect and is mediated by transmembrane receptors [29]. In normal cells, the transmembrane receptor binds to the molecular chaperone in the endoplasmic reticulum cavity to remain inactive. When stress occurs, the molecular chaperone and transmembrane receptors are dissociated, resulting in receptor activation and induction of ERS. However, when the protective effect of the endoplasmic reticulum occurs with an overly compensatory reaction, it becomes the trigger point of apoptosis signaling, which promotes the expression of apoptosis-inducing factors, such as caspase-12 and CHOP [30]. Therefore, in the process of BM-MSC apoptosis, it is important to identify the expression of caspase-12 and CHOP because they are involved in ERS. We demonstrated that the expression of caspase-12 and CHOP increased during BM-MSC apoptosis, suggesting that ERS is involved in the apoptosis of BM-MSCs.

We also detected changes in the MAPK signaling pathway during BM-MSC apoptosis. Previous studies have shown that this signaling pathway is involved in a variety of physiological processes, such as cell movement, apoptosis, differentiation and growth and proliferation [20, 21]. Therefore, we hypothesized that the three MAPK pathways of p-38, JNK and ERK also regulate the apoptosis of BM-MSCs, and our results also showed that the three pathways were involved in the apoptosis of BM-MSCs. To further investigate the MAPK signaling pathway in BM-MSCs, apoptosis plays an important role, rather than an incidental phenomenon, so we used SB202190, SP600125 and PD98059 to block the p-38, JNK and ERK signaling pathways, respectively, to observe the changes in BM-MSCs under hypoxic conditions. We found that the apoptotic rate of BM-MSCs decreased after the p-38 or JNK pathways were blocked, indicating that the p-38 and JNK pathways promoted the apoptosis of BM-MSCs under H/SD conditions. After the ERK pathway was blocked, the apoptotic rate of BM-MSCs increased compared with the H/SD group, indicating that the ERK pathway plays an important role in the process of anti BM-MSC apoptosis.

To further investigate whether there is a correlation between the MAPK signaling pathway and ERS in the regulation of BM-MSC apoptosis, we used SB202190 and SP600125 to block p-38 and the JNK signaling pathway to observe the expression of caspase-12, procaspase-12 and CHOP, respectively. Procaspase-12, as the precursor of caspase-12, can form caspase-12 with apoptotic activity after being sheared [31, 32]. Ours is the first evidence suggesting that the expression of caspase-12 decreased significantly after SB202190 blocked p-38, proving that p-38 is upstream of the caspase-12 signal. Further, when the p-38 signal pathway was blocked, the expression level of procaspase-12 increased, indicating that blocking the p-38 signaling pathway interfered with the activation of caspase-12. Therefore, the mechanism of SB202190 inhibiting BM-MSC apoptosis might be due to the inhibition of the p-38 signaling pathway, which blocks the protein maturation process of procaspase-12 to caspase-12, thereby reducing the apoptosis of cells. Unfortunately, the relationship between the p-38 signaling pathway and CHOP, as well as the relationship between the JNK signaling pathway and ERS, is not clear.

In conclusion, our results in this study showed that the mechanism of BM-MSC apoptosis involves the MPAK signaling pathway and endoplasmic reticulum stress. Among these factors, p-38, JNK, CHOP and caspase-12 play important roles in promoting the apoptosis of BM-MSCs, while ERK is contrary to other signals, playing a role in the anti-apoptosis of BM-MSCs. In addition, we further demonstrated that the p-38-caspase-12 signaling pathway was activated in the absence of serum and hypoxia to promote the apoptosis of BM-MSCs. Our results provided some evidence for the mechanism of BM-MSC apoptosis caused by hypoxia and serum deprivation, and they also provided a reference point for the selection of anti-apoptotic targets of BM-MSCs. Moreover, our research established four hypoxia time points for the BM-MSC apoptosis model and screened out the time point with the highest rate of apoptosis, that is, H/SD 6 h, providing reference data for the establishment of the BM-MSC apoptosis model.

Acknowledgements

This study was supported by the Hangzhou Health Science and Technology Project (2017-Z10) and the Hangzhou Science and Technology Bureau Project (20150733Q57, 20160533B63).

Disclosure of conflict of interest

None.

Address correspondence to: Dr. Tielong Chen, Department of Cardiology, Hangzhou Hospital of Traditional Chinese Medicine, No. 453 Stadium Road, Hangzhou 310007, China. E-mail: ctlppp@163.com; Dr. Houyong Zhu, Department of Cardiology, Hangzhou Hospital of Traditional Chinese Medicine, Hangzhou Dingqiao's Hospital, Hangzhou 310007, China. E-mail: houyongzhu@foxmail.com

References

[1] Gheorghiade M and Bonow RO. Chronic heart failure in the United States: a manifestation of coronary artery disease. Circulation 1998; 97: 282-289.

[2] Cicenia M, Fedele F, Petronilli V, De Carlo C, Moscucci F, Schina M and Sciomer S. Hidden

in the heart: a peculiar type of left ventricular remodeling after acute myocardial infarction. Echocardiography 2017; 34: 1738-1739.
[3] Mao Y, Koga JI, Tokutome M, Matoba T, Ikeda G, Nakano K and Egashira K. Nanoparticle-mediated delivery of pitavastatin to monocytes/macrophages inhibits left ventricular remodeling after acute myocardial infarction by inhibiting monocyte-mediated inflammation. Int Heart J 2017; 58: 615-623.
[4] Fujisue K, Sugamura K, Kurokawa H, Matsubara J, Ishii M, Izumiya Y, Kaikita K and Sugiyama S. Colchicine Improves survival, left ventricular remodeling, and chronic cardiac function after acute myocardial infarction. Circ J 2017; 81: 1174-1182.
[5] Natsumeda M, Florea V, Rieger AC, Tompkins BA, Banerjee MN, Golpanian S, Fritsch J, Landin AM, Kashikar ND, Karantalis V, Loescher VY, Hatzistergos KE, Bagno L, Sanina C, Mushtaq M, Rodriguez J, Rosado M, Wolf A, Collon K, Vincent L, Kanelidis AJ, Schulman IH, Mitrani R, Heldman AW, Balkan W and Hare JM. A combination of allogeneic stem cells promotes cardiac regeneration. J Am Coll Cardiol 2017; 70: 2504-2515.
[6] Xu JY, Cai WY, Tian M, Liu D and Huang RC. Stem cell transplantation dose in patients with acute myocardial infarction: a meta-analysis. Chronic Dis Transl Med 2016; 2: 92-101.
[7] Reinsch M and Weinberger F. [Stem cell-based cardiac regeneration after myocardial infarction]. Herz 2018; 43: 109-114.
[8] Guadix JA, Orlova VV, Giacomelli E, Bellin M, Ribeiro MC, Mummery CL, Perez-Pomares JM and Passier R. Human pluripotent stem cell differentiation into functional epicardial progenitor cells. Stem Cell Rep 2017; 9: 1754-1764.
[9] Shafei AE, Ali MA, Ghanem HG, Shehata AI, Abdelgawad AA, Handal HR, Talaat KA, Ashaal AE and El-Shal AS. Mesenchymal stem cell therapy: a promising cell-based therapy for treatment of myocardial infarction. J Gene Med 2017; 19.
[10] Zhang M, Liu D, Li S, Chang L, Zhang Y, Liu R, Sun F, Duan W, Du W, Wu Y, Zhao T, Xu C and Lu Y. Bone marrow mesenchymal stem cell transplantation retards the natural senescence of rat hearts. Stem Cells Transl Med 2015; 4: 494-502.
[11] Kan CD, Lee HL and Yang YJ. Cell transplantation for myocardial injury: a preliminary comparative study. Cytotherapy 2010; 12: 692-700.
[12] Zarbakhsh S, Moradi F, Joghataei MT, Bahktiari M, Mansouri K and Abedinzadeh M. Evaluation of the functional recovery in sciatic nerve injury following the co-transplantation of schwann and bone marrow stromal stem cells in rat. Basic Clin Neurosci 2013; 4: 291-298.
[13] Meng Y, Ji J, Tan W, Guo G, Xia Y, Cheng C, Gu Z and Wang Z. Involvement of autophagy in the procedure of endoplasmic reticulum stress introduced apoptosis in bone marrow mesenchymal stem cells from nonobese diabetic mice. Cell Biochem Funct 2016; 34: 25-33.
[14] Zhang Z, Yang M, Wang Y, Wang L, Jin Z, Ding L, Zhang L, Zhang L, Jiang W, Gao G, Yang J, Lu B, Cao F and Hu T. Autophagy regulates the apoptosis of bone marrow-derived mesenchymal stem cells under hypoxic condition via AMP-activated protein kinase/mammalian target of rapamycin pathway. Cell Biol Int 2016; 40: 671-685.
[15] Minchenko OH, Tsymbal DO, Minchenko DO and Ratushna OO. The role of the TNF receptors and apoptosis inducing ligands in tumor growth. Ukr Biochem J 2016; 88: 18-37.
[16] Motegi SI, Sekiguchi A, Uchiyama A, Uehara A, Fujiwara C, Yamazaki S, Perera B, Nakamura H, Ogino S, Yokoyama Y, Akai R, Iwawaki T and Ishikawa O. Protective effect of mesenchymal stem cells on the pressure ulcer formation by the regulation of oxidative and endoplasmic reticulum stress. Sci Rep 2017; 7: 17186.
[17] Kong FJ, Ma LL, Guo JJ, Xu LH, Li Y and Qu S. Endoplasmic reticulum stress/autophagy pathway is involved in diabetes-induced neuronal apoptosis and cognitive decline in mice. Clin Sci (Lond) 2018; 132: 111-125.
[18] Zhao YL, Li F, Liu YW, Shi YJ, Li ZH, Cao GK and Zhu W. Adiponectin attenuates endoplasmic reticulum stress and alveolar epithelial apoptosis in COPD rats. Eur Rev Med Pharmacol Sci 2017; 21: 4999-5007.
[19] Liu L, Zhang Y, Wang Y, Peng W, Zhang N and Ye Y. Progesterone inhibited endoplasmic reticulum stress associated apoptosis induced by interleukin-1beta via the GRP78/PERK/CHOP pathway in BeWo cells. J Obstet Gynaecol Res 2018; 44: 463-473.
[20] Bryk D, Olejarz W and Zapolska-Downar D. [Mitogen-activated protein kinases in atherosclerosis]. Postepy Hig Med Dosw (Online) 2014; 68: 10-22.
[21] Lawan A and Bennett AM. Mitogen-activated protein kinase regulation in hepatic metabolism. Trends Endocrinol Metab 2017; 28: 868-878.
[22] Lake D, Correa SA and Muller J. Negative feedback regulation of the ERK1/2 MAPK pathway. Cell Mol Life Sci 2016; 73: 4397-4413.
[23] Zhu H, Ding Y, Xu X, Li M, Fang Y, Gao B, Mao H, Tong G, Zhou L and Huang J. Prostaglandin E1 protects coronary microvascular function via the glycogen synthase kinase 3beta-mitochondrial permeability transition pore pathway in

rat hearts subjected to sodium laurate-induced coronary microembolization. Am J Transl Res 2017; 9: 2520-2534.
[24] Herr I, Wilhelm D, Meyer E, Jeremias I, Angel P and Debatin KM. JNK/SAPK activity contributes to TRAIL-induced apoptosis. Cell Death Differ 1999; 6: 130-135.
[25] Frasch SC, Nick JA, Fadok VA, Bratton DL, Worthen GS and Henson PM. p38 mitogen-activated protein kinase-dependent and -independent intracellular signal transduction pathways leading to apoptosis in human neutrophils. J Biol Chem 1998; 273: 8389-8397.
[26] Sanchez-Perez I, Murguia JR and Perona R. Cisplatin induces a persistent activation of JNK that is related to cell death. Oncogene 1998; 16: 533-540.
[27] Shirzeyli MH, Khanlarkhani N, Amidi F, Shirzeyli FH, Aval FS and Sobhani A. Bones Morphogenic Protein-4 and retinoic acid combined treatment comparative analysis for in vitro differentiation potential of murine mesenchymal stem cells derived from bone marrow and adipose tissue into germ cells. Microsc Res Tech 2017; 80: 1151-1160.
[28] Klopsch C, Skorska A, Ludwig M, Gaebel R, Lemcke H, Kleiner G, Beyer M, Vollmar B, David R and Steinhoff G. Cardiac mesenchymal stem cells proliferate early in the ischemic heart. Eur Surg Res 2017; 58: 341-353.
[29] Demirtas L, Guclu A, Erdur FM, Akbas EM, Ozcicek A, Onk D and Turkmen K. Apoptosis, autophagy & endoplasmic reticulum stress in diabetes mellitus. Indian J Med Res 2016; 144: 515-524.
[30] Wang MG, Li WH, Wang XY, Yang DB, Wang ZY and Wang L. CaMKII is involved in subcellular Ca (2+) redistribution-induced endoplasmic reticulum stress leading to apoptosis in primary cultures of rat proximal tubular cells exposed to lead. Oncotarget 2017; 8: 91162-91173.
[31] Badiola N, Penas C, Minano-Molina A, Barneda-Zahonero B, Fado R, Sanchez-Opazo G, Comella JX, Sabria J, Zhu C, Blomgren K, Casas C and Rodriguez-Alvarez J. Induction of ER stress in response to oxygen-glucose deprivation of cortical cultures involves the activation of the PERK and IRE-1 pathways and of caspase-12. Cell Death Dis 2011; 2: e149.
[32] Jiang S, Xie Q, Zhou H, Zhang W, Zhou X, Li G, Shi Y and Jin Y. Ribozyme-mediated inhibition of caspase-12 activity reduces apoptosis induced by endoplasmic reticulum stress in primary mouse hepatocytes. Int J Mol Med 2008; 22: 717-724.